ROYAL SOCIETY OF CHEMISTRY

Nanoscale

Exploiting the tetrazine-norbornene reaction for single polymer chain collapse

SCHOLARONE™
Manuscripts

ARTICLE TYPE

Exploiting the tetrazine-norbornene reaction for single polymer chain collapse

Claire F. Hansell[a], Annhelen Lu[a], Joseph P. Patterson[a] and Rachel K. O'Reilly*[a]

Single chain polymer nanoparticles (SCNPs) have been formed using polystyrenes decorated with pendent norbornenes and a bifunctional tetrazine crosslinker. Characterisation by size exclusion chromatography and ^{1}H NMR gives evidence for the formation of SCNPs by the tetrazine-norbornene reaction, whilst light scattering, neutron scattering, transmission electron microscopy and atomic force 10 microscopy show that discrete well-defined nanoparticles are formed and their size in solution calculated.

With the increasing sophistication of 'nano' chemistry, it is desirable that molecules or particles of any possible size, morphology and functionality can be synthesised. 'Bottom-up' 15 techniques such as single molecule dendrimer synthesis give access to molecules up to approximately 5 nm in size,[1] and 'top-down' approaches such as self-assembly of amphiphiles or mini-emulsion polymerisations give access to macromolecular constructs down to around 20 nm. However, particles of a size 20 range 5–20 nm have traditionally been difficult to access. Such particles are useful for, amongst other things, semiconductor lithography[2] and as sacrificial porogens.[3] This size range has, however, been achieved using the collapse of single polymer chains to form soft, defined nanoobjects, or single chain polymer 25 nanoparticles (SCNPs). The first example of this used a radical initiator to radically crosslink pendent acrylate functionalities along a polycaprolactone or polymethylmethacrylate backbone under ultradilute conditions.[3] Since then, the development of a slow addition method has resulted in the ability to feasibly 30 synthesise SCNPs on a larger scale,[4] and as such a variety of crosslinking methods have been used in SCNP synthesis. These include the high temperature self-condensation of benzocyclobutene (BCB),[5,6] benzoxazines[7,8] and sufonyl azides.[9] Negating the need for high reaction temperatures, polymerisation 35 of alkyne- and azide-containing monomers into a single chain also enabled the use of the room temperature Cu(I) catalysed reaction between an azide and terminal alkyne for SCNP formation,[10-12] and using only alkyne-containing monomers achieved the same result using Glaser-Hay coupling of alkynes.[13] UV-induced 40 photodimerisation of coumarin[14] and cinnamyl[15] groups, and photo-induced Bergman cyclisations[16-18] have also been employed to circumvent the need for boiling solvents. Alkene metathesis,[19] crosslinking of isocyanates with amines,[20] and oxidative polymerisation of thiophene-type pendent monomers[21] have also 45 been used for SCNP formation. Whilst an array of methods have been shown to facilitate SCNP formation, all require a degree of experimental difficulty. The isocyanate-amine method, whilst

carried out under mild conditions with no added catalyst, suffers from extremely poor incidental water tolerance, and the other 50 methods listed all require additional catalysts or special experimental conditions of varying complexity to work efficiently.

The tetrazine-norbornene (Tz-Nb) reaction is fast, high-yielding and easily carried out, requiring no special experimental 55 conditions, additional catalyst or stimulus to proceed to near-quantitative conversions at room temperature,[22-26] thus making it an ideal candidate for the formation of SCNPs. Indeed, in recent years the Tz-Nb reaction has been used to both modify and conjugate polymer chains,[27,28] functionalise micelles,[29] 60 fluorescently tag live cells in a variety of biomedical applications,[30-32] and functionalise DNA.[33] In this work, we aim to use the Tz–Nb reaction as it has some advantages to those reactions previously used for SCNP formation. The high-temperature reactions such as the BCB reactions preclude 65 incorporation of many functionalities, should the basic SCNP structure be utilised to generate more complex frameworks, so the room temperature nature of the Tz–Nb reaction is advantageous in that respect. The tetrazine and norbornene functionalities, whilst reactive and by extension not stable under *all* conditions, are 70 stable enough that SCNP formation does not have to be run under stringently anhydrous or anaerobic conditions. Furthermore, the Nb functionalities can be readily incorporated into a polymer by reversible addition fragmentation chain transfer (RAFT) polymerisation,[34] and thus the number of synthetic steps is 75 reduced relative to the SCNP precursors that require post-polymerisation modification to incorporate the reactive functionalities prior to SCNP formation. The catalyst- and additive-free nature of the Tz–Nb reaction, with no by-products aside from N_2 gas evolved, also simplifies SCNP synthesis and 80 their subsequent purification.

Results and Discussion

A tetrazine crosslinnker **Tz-Tz** was synthesised using a

bifunctional acyl chloride and alcohol-functionalised tetrazine.[35] **Tz-Tz** was obtained in moderate yield (38%) as a pink solid, and identity and purity confirmed by ^{1}H and ^{13}C NMR spectroscopies (Figure S1), HRMS and IR spectroscopy. To form the precursor

Figure 1. Formation of polystyrene SCNPs using Tz-Nb crosslinking. The adduct formed is likely to be a mixture of dihydropyradizine isomers and pyradizines, for clarity only the pyradizine adduct is shown.
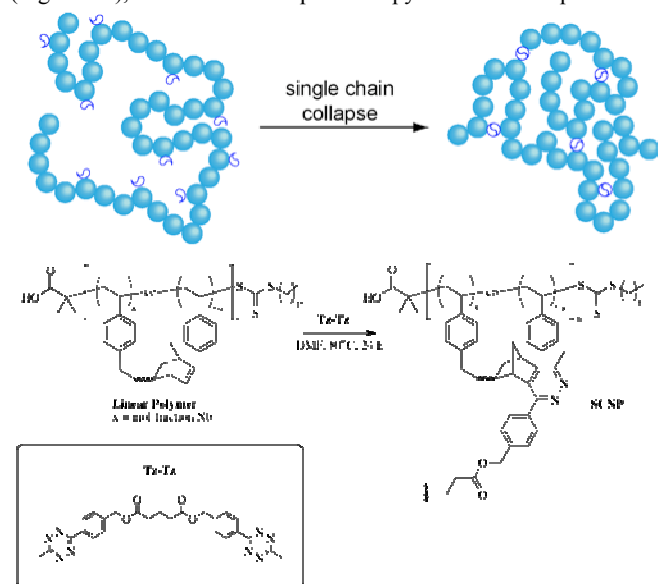
polymers to the SCNPs, linear poly(styrene)s of varying molecular weights and containing 5-20 mol% pendent Nb groups were synthesised by RAFT polymerisation methods according to literature precedents.[26, 36]

SCNP formation was carried out by the 'slow addition'[4] method rather than the 'ultradilute'[3] method; briefly, a solution of linear polymer in DMF ($[Nb]$ = 0.01 M, calculated according to the method of Hawker *et al.*,[3] and as such the polymer concentration varied with polymer molecular weight and mol% Nb) was added at 1 mL/h to a stirred solution of **Tz-Tz** crosslinker (0.5 eq. per Nb unit on the linear polymer, such that the ratio of Tz and Nb units was equimolar) in DMF at 80 °C (Figure 1). DMF was chosen as the solvent due to its ability to solubilise both the crosslinker and polystyrene-based linear copolymers, but as it is not an ideal solvent for polystyrene it was hypothesised that the linear chains would be relatively collapsed prior to crosslinking and that this would facilitate SCNP formation by bringing Nb units on the same chain into closer proximity than in an ideal/theta solvent. Despite anticipating that the reaction would proceed fast enough at room temperature, initial trials at room temperature were surprisingly unsuccessful; qualitatively the colour change from pink to orange indicative of a successful reaction did not occur within 24 hours and only gelled polymer was obtained when drying the reaction mixture for analysis. This is indicative of a reaction rate not sufficiently fast for SCNP formation. In an effort to speed the reaction at room temperature, faster rates of addition of the linear polymer to **Tz-Tz** solution were attempted. These resulted in pronounced polymer–polymer coupling, evidenced by significant high M_w shoulders in the SEC traces compared to the parent linear polymer, some decreases in M_n were also observed, showing that some SCNP formation was occurring. Whilst reaction at room temperature was unsuccessful, increasing the

temperature to 80 °C facilitated a fast enough Tz-Nb reaction for SCNP formation to occur. Table 1 shows the SEC results of the SCNPs with respect to their linear precursors (**P1-9**) of varying molecular weights and Nb incorporations. Smaller polymers (< 5 kDa, data not included) were also used, however these did not exhibit shifts in the SEC traces, and we attribute this to the low number of available Nb groups which did not enable crosslinking in multiple places on a single polymer chain.

Table 1. Apparent molecular weight properties of linear polymers and formed SCNPs measured by SEC (THF eluent)

| Entry | Mol% Nb[a] | Linear Precursor | | | | SCNP | | | |
		M_p / kDa[b]	M_n / kDa[b]	M_w / kDa[b]	$Đ_M$[b]	M_p / kDa[b]	M_n / kDa[b]	M_w / kDa[b]	$Đ_M$[b]
P1	20	45.8	34.1	62.3	1.83	16.3	11.7	17.7	1.50
P2	10	50.5	44.3	55.3	1.25	22.0	14.9	23.9	1.60
P3	5	41.6	31.3	43.5	1.35	33.2	25.5	47.5	1.86
P4	20	28.0	21.6	36.0	1.67	14.9	12.0	18.3	1.52
P5	10	19.1	15.7	19.9	1.27	17.6	16.3	24.1	1.48
P6	5	31.3	23.9	31.5	1.32	25.2	21.5	41.2	1.91
P7	20	10.4	8.8	10.8	1.23	7.4	6.5	7.9	1.21
P8	10	14.1	13.3	17.3	1.31	12.6	11.8	17.2	1.46
P9	5	10.1	9.1	10.5	1.16	9.4	9.5	13.8	1.45

[a] Mol% Nb calculated from monomer feed ratio in linear precursor synthesis. [b] M_p, M_n, M_w and $Đ_M$ calculated relative to PS standards

In order to rule out the possibility that the observed changes in apparent molecular weight are in fact due to changes in hydrophobicity due to the Tz-Nb reaction, a model polymer was synthesised. This model polymer **P0** was formed by the reaction of linear **P1** with a monofunctional tetrazine (**Tz-COOEt**), analogous to half of the Tz-Tz crosslinker (Scheme S1). No significant difference was observed between the SEC trace of **P0** and simply heating linear **P1** at 80 °C for 24 h in DMF (Figure S3), therefore we can conclude that shifts in the apparent molecular weights from the linear polymer upon reaction with the crosslinker **Tz-Tz** are indeed due to SCPN formation. It should be noted, however, that the highest MW linear polymers with 10 and 20 mol% Nb incorporation did in fact display a very slight shift in apparent M_n and M_w when heated in DMF at 80 °C for 24 h with no crosslinker or monofunctional tetrazine present, but it was not a large change (*ca.* 4-6 kDa in M_n) compared to those detailed in Table 1. This phenomenon was accompanied by a reduction in the intensity of the UV/vis signal at 309 nm arising from the RAFT end group. Thus we hypothesise that the small shift may be a result of some incidental degradation of the RAFT group to a thiol, which then reacts with a Nb unit on the backbone, essentially forming extraneous cycles in some polymer chains. However, this reaction we propose is not detrimental to the overall formation of SCNPs because the backbiting of the terminal thiol onto a pendent Nb is analogous to crosslinking two pendent Nb groups and therefore could be considered part of the SCNP-forming process. The only detrimental case is when a terminal thiol reacts with a Nb group on an adjacent polymer chain, forming polymer-polymer coupled species which present as a small high molecular weight shoulder in the resulting SEC trace.

Inspecting the results of the SEC measurements in Table 1 in the majority of cases there is an observed decrease in the apparent M_n and M_w values, which is exactly as would be expected and from which we are able to infer successful SCNP formation.[37]

However, these decreases are mitigated, and in some cases — especially lower mol% Nb incorporations — negated by the appearance of a high molecular weight shoulder in the SEC traces. As this was also observed in the control polymer **P0** described in
5 the previous paragraph, it was decided that this was not a feature peculiar to SCNP formation, but rather the result of heating the RAFT-synthesised polymer for 24 h and resulting in RAFT trithiocarbonate degradation and subsequent thiol-Nb coupling described above. In all cases, the decrease in M_p, rather than M_w
10 or M_n, from the linear polymer to SCNP gives a qualitative indication of successful SCNP formation. Polymers **P1**, **P4** and **P7** (20 mol% Nb) showed the greatest proportional decreases in M_p, which correlates to the SCNPs formed being crosslinked to the greatest degree and therefore the hydrodynamic size change from
15 the linear polymer to SCNP being the most pronounced in the SEC measurements. The 10 mol% Nb-containing polymers show a lower proportional change in molecular weight, followed by the 5 mol% Nb-containing polymers, but as a shift in molecular weight is still observed, we can infer that 5 mol% Nb is enough to
20 result in successful SCNP formation.

^{1}H NMR spectroscopy in CDCl$_3$ showed complete reaction of the Nb units (linear and SCNP **P1** shown in Figure 3) as evidenced by the lack of signal at 6.0 ppm. This was not expected, as molecular simulations[38] and experimental evidence[20] has shown that after a
25 certain degree of crosslinking, some reactive groups become inaccessible and so remain unreacted. In this instance, either all Nb groups have reacted, or else the introduction of aromatic groups by the crosslinker may have deshielded any signals arising from unreacted Nb further, such that they are subsumed into the
30 broad aromatic signals.
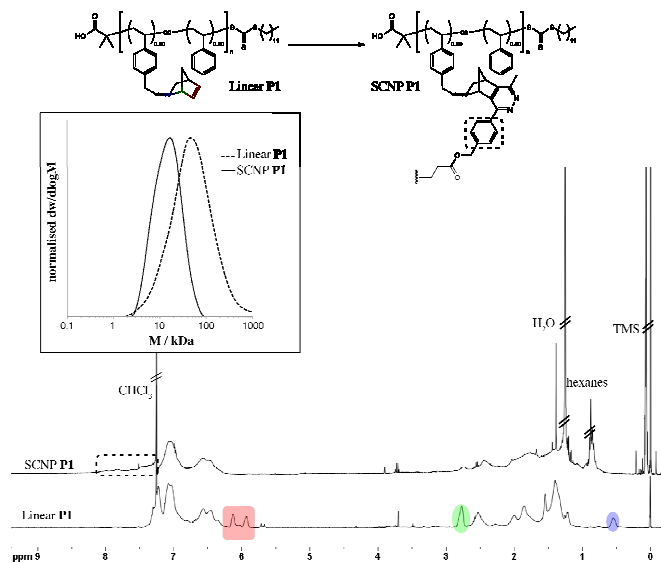
Figure 2. ^{1}H NMR spectra (400 MHz, CDCl$_3$) of linear precursor and SCNP **P1**, key Nb signals lost upon crosslinking with **Tz-Tz** highlighted in red, green and blue, and signals arising from the aromatic part of the
35 crosslinker highlighted with a dotted line.

Having inferred from SEC analysis that successful SCNP formation had occurred across a range of molecular weights, and that this occurred *via* Tz-Tz crosslinking of the Nb groups from ^{1}H NMR spectroscopy, we carried out further analysis, in both the
40 dry state and in solution, on SCNP **P1** to confirm that discrete SCNPs were indeed being formed, and to determine their size. AFM analysis of SCNP **P1**, drop-deposited from a CH$_2$Cl$_2$ solution at 1 µg/mL (Figure 3 and S4) revealed a relatively uniform distribution of SCNPs on the mica surface, characteristic
45 of SCNP formation[27] and in contrast to AFM analysis of both the linear polymer (Figure S5) in which only featureless (text obscured) on the surface of the mica (Figure S3).
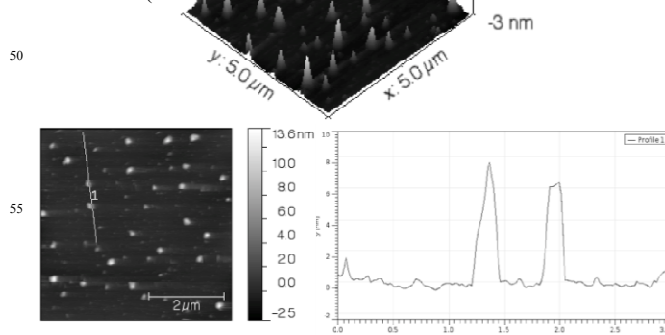
65 **Figure 3.** AFM Z-height image (top) and plot profile (bottom) of SCNP **P1**

The SCNP **P1** particles showed an average (over at least 100 particles) height differential from the particle peak to the mica surface of 5.8 nm. Particle width data extrapolated from AFM
70 suffers from significant inaccuracies due to tip convolution effects and as such was disregarded. TEM imaging on graphene oxide (GO)[39] revealed distinct particles (Figure S6), and greyscale plots were employed to calculate the diameter of the SCNPs from the TEM images (Figure S7). Counting 100 particles, this gave an
75 average particle diameter of 15.8 nm. In order to extrapolate the radius of the SCNPs in solution from the hemispherical particles dried to the AFM and TEM substrates, we combined the height information from AFM (h_{av} = 5.8 nm) with the diameter information from TEM (D_{av} = 15.8 ± 5.5 nm) to find the SCNP
80 volume. Calculating the radius from the SCNP volume gave a SCNP radius in solution of 5.7 nm for entry **P1**.

SANS analysis of SCNP **P1** (10 mg/mL in THF-d$_8$) further corroborated the formation of soft fractal nanoobjects from the linear counterpart, as demonstrated by the change from a linear to
85 asymptotic Kratky plot, and the slight change in gradient of a log-log plot in the Porod region (Figure S10). A Guinier plot (Figure S11) revealed an unexpectedly large R_g value of 12.0 nm, which is significantly larger than the extrapolated R_h value (5.7 nm) calculated by combining AFM and TEM measurements.
90 Calculation of the R_h values by DLS at 20 °C across a range of concentrations (0.01 - 10 mg/mL in CHCl$_3$) also resulted in values that were consistently larger than the precursor linear **P1** (linear **P1** *ca.* 3-4 nm, SCNP **P1** *ca.* 6-10 nm, concentration dependent). However, upon heating the solution above room temperature, the
95 size distribution was resolved into two distinct populations, (Figure S12) approximately equal in number of particles, and of R_h ~ 3 and 7 nm. Thus we hypothesise that there is a tendency for

the SCNPs to aggregate, and that these aggregates are only broken up by heating. If this were the case, then the actual R_h of a single SCNP is calculated to be the R_h of the smaller of the two populations, and is 3.7 nm. This also means that the SANS data measured at 20 °C measured the R_g of aggregated species rather than single SCNPs and provides some explanation for the unusually large R_g value obtained. Molecular weight calculation of SCNP **P1** at 20 °C 10 mg/mL in CHCl$_3$) by light scattering also corroborated the aggregation theory, as the calculated M_w was 227 kDa, in comparison to linear **P1** = 62.3 kDa (by SEC) and control **P0** = 79.2 kDa. The expected M_w value for a single SCNP is one very close to the M_w of the linear precursor, as the only change in atomic structure is the addition of crosslinkers and the concomitant loss of N$_2$ as a by-product. The fact that the obtained M_w for SCNP **P1** was between 2 and 3 times that of the linear precursor suggests that at 20 °C, 2-3 linear chains are aggregated together. Whether this is in one nanoparticle containing 2-3 interconnected chains or 2-3 separate SCNPs aggregated, this light scattering data is unable to show, but the temperature dependence of the DLS data discussed above suggests that SCNPs are indeed being formed and then subsequently aggregating, which can be broken up by heating.

Experimental

Materials and Methods

All chemicals and reagents were purchased from Sigma-Aldrich and used without further purification unless otherwise stated. Styrene (St) was distilled over CaH$_2$, 2,2′-Azobis(2-methylpropionitrile) (AIBN) was recrystallised twice from methanol and both were stored at 4 °C in the dark before use.

Nuclear magnetic resonance (^{1}H and ^{13}C NMR) spectra were recorded at 400 or 500 MHz in CDCl$_3$ or DMSO-d_6 solution at 20 °C on a Bruker DPX-400 or Bruker AM-500 spectrometer. Chemical shifts are reported as δ in parts per million (ppm) and referenced to the chemical shift of the residual solvent resonances (CDCl$_3$ ^{1}H: δ = 7.26 ppm; ^{13}C δ = 77.16 ppm; DMSO-d_6 ^{1}H: δ = 2.50 ppm; ^{13}C δ = 39.52 ppm). Coupling constants (J) are given in Hz. The resonance multiplicities are described as s (singlet), d (doublet), app t (apparent triplet), q (quartet) or m (multiplet). For acquired ^{13}C NMR experiments, multiplicities were distinguished using an ATP pulse sequence whereby methylene and quaternary carbon signals appear 'up' (u) and methyl and methane carbons 'down' (dn). Diffusion ordered spectra were acquired using the standard Bruker 2D sequence for diffusion measurements using stimulated echo and LED, and processed using Bruker Topspin and DOSY Toolbox softwares, assuming a single population of molecules.

Molar mass distributions were measured using size exclusion chromatography (SEC), and all samples were filtered through 0.22 μm PTFE filters before injection. Analyses were performed in HPLC grade THF containing 2 vol% triethyl amine (TEA), dimethylacetamide (DMAc) or CHCl$_3$ at 30 °C, at a flow rate of 1.0 mL/min on a set of two PLgel 5 μm Mixed-D columns and one PLgel 5 μm guard column with differential refractive index detection. Polystyrene standards were used for calibration, samples were injected using a PL AS RT autosampler and molecular weight and dispersity indices determined using Cirrus software.

FT-IR spectra were obtained using a Perkin Elmer Spectrum 100 FT-IR. 16 scans from 600 to 4000 cm^{-1} were taken, and the spectra corrected for background absorbance.

UV/vis measurements were made on a Perkin Elmer Lambda 35 UV/vis spectrometer, far UV quartz cuvettes (Hellma) were used. Hydrodynamic diameters (D_h) and size distributions of SCNPs were determined by DLS on a Malvern Zetasizer Nano ZS operating at 20 °C with a 4 mW He-Ne 633 nm laser module. Samples were filtered through a 0.45 μm PTFE filter prior to measurement and quartz cuvettes were used. Measurements were made at a detection angle of 173° (back scattering), and the data analysed using Malvern DTS 6.20 software, using the multiple narrow modes setting. All measurements were made in triplicate, with 10 runs per measurement. To discount small amounts of aggregates/larger structures in the solutions, which skew the automatically generated results from the Zetasizer, the data were reanalysed by fitting the correlation functions to a stretched exponential function (Kohlrausch-Williams-Watts) from which the relaxation time was derived for the major population, and from this the R_h (and therefore D_h) was calculated using the Stokes-Einstein equation.

SLS measurements were performed at angles from 30° up to 150° with an ALV CGS3 (λ = 632 nm) and at 25 ± 1 °C. The data were collected with 100 s run time in duplicate, calibration was with filtered toluene and the background was measured with filtered CHCl$_3$. The refractive index increment of the polymers in chloroform was assumed to be equal to that of polystyrene (0.15 mL/g).

TEM analyses were performed on a JEOL 2011 (LaB$_6$) microscope operating at 200 kV, equipped with a GATAN UltraScan 1000 digital camera. Conventional bright field conditions were used to image samples in all cases. TEM grids used were lacey carbon-coated copper grids (Agar Scientific, 400 mesh, S116-4) coated with a thin layer of graphene oxide. SCNP solutions were diluted to 2.5 mg/mL in CH$_2$Cl$_2$ before 4 μL of each sample was drop-deposited onto the graphene oxide-coated grids, blotted immediately and allowed to air dry. No subsequent staining or treatment of the grids was required prior to imaging the samples.[39] Images were analysed using ImageJ software, and 50 particles were measured to produce a mean and standard deviation for the particle size (D_{av}).

AFM images were taken in tapping mode on a Multimode AFM with Nanoscope IIIA controller with Quadrex. Silicon AFM tips were used with nominal spring constant and resonance frequency of 3.5 Nm^{-1} and 75 kHz (MikroMasch NSC18). Samples were diluted to 0.001 mg/mL in CH$_2$Cl$_2$ and 4 μL drop-deposited onto freshly cleaved mica discs (9.9 mm, Agar Scientific G250-6). Data were processed and analysed using Gwyddion software.

SANS experiments were performed on the ISIS neutron beam facility, sans2d instrument at the Rutherford Appleton Laboratory, Oxford. Samples were measured at 10 mg/mL in THF-d$_8$ – a good solvent for polystyrene and one that provides a suitably high contrast in scattering length to the polymer.

Syntheses

As described in a literature precedent,[36] the requisite amounts of styrene and Nb–St, DDMAT and AIBN (1:0.1 [DDMAT]:[AIBN]) were dissolved in toluene (1:1 ^{w}/$_v$) and

subjected to four freeze-evacuate-thaw cycles. The polymerisation ampoule was warmed to room temperature under nitrogen and then immersed in an oil bath at 70 °C for 23–24 h. Monomer conversions were determined by ^{1}H NMR to be 30-40% for all polymers, and the polymer was precipitated 3 times from cold methanol and 3 times from cold pentane before being freeze dried from dioxane and recovered as a yellow or white powdery solid.

[p-(6-Methyl-1,2,4,5-tetrazin-3-yl)phenyl]methanol (Tz–OH)

Tz–OH was synthesised according to a modified literature procedure.[35] 4-Hydroxymethyl benzonitrile (1.00 g, 7.51 mmol), nickel triflate (1.34 g, 3.76 mmol), acetonitrile (3.92 mL, 75.1 mmol) and hydrazine monohydrate (18.3 mL, 376 mmol) were mixed in a sealed ampoule and stirred at RT for 30 min to ensure complete dissolution of all the reagents. The ampoule was placed in an oil bath at 60 °C for 24 h behind a blast shield, after which it was allowed to cool to room temperature and opened carefully due to the pressure build-up during the reaction. The resulting brown mixture was added to sodium nitrite (5.18 g, 75.1 mmol) in 20 mL water, after which conc. HCl was added extremely slowly, diluting with water as necessary (final volume *ca.* 500 mL) to control the resulting effervescence and being careful of the evolved nitrous gases, until pH 3 was reached. The aqueous phase was extracted with EtOAc (3 x 200 mL), then the organic phase washed with H_2O and brine and dried over $MgSO_4$. The product was isolated by flash column chromatography (2:1 hexanes:EtOAc, R_f 0.15) as a pink solid (374 mg, 13% yield). ^{1}H NMR (400 MHz, $CDCl_3$) δ (ppm): 8.57 (2H, d, $J = 8.2$ Hz), 7.58 (2H, d, $J = 8.2$ Hz), 4.83 (2H, s), 3.09 (3H, s). ^{13}C NMR (100 MHz, $CDCl_3$) δ (ppm): 167.4 (u), 164.1 (u), 145.8 (u), 131.1 (u), 128.3 (dn), 127.6 (dn), 64.9 (u), 21.3 (dn).

Di[p-(6-methyl-1,2,4,5-tetrazin-3-yl)phenyl]methyl glutarate (Tz–Tz)

Tz–OH (336 mg, 1.66 mmol) was dissolved in dry CH_2Cl_2 (15 mL) under a N_2 atmosphere, and glutaryl chloride (106 μL, 141 mg, 0.831 mmol) added *via* syringe. The mixture was stirred at room temperature for 24 h, the solvent removed *in vacuo* and the product isolated by flash column chromatography (2% MeOH in CH_2Cl_2, R_f 0.6) as a pink solid (315 mg, 0.629 mmol, 38% yield). HRMS (ESI, [M+H]$^+$) *m/z*: predicted 501.1999, found 501.1997. ^{1}H NMR (400 MHz, $CDCl_3$) δ (ppm): 8.57 (d, $J = 8.4$ Hz, 4H), 7.55 (d, $J = 8.4$ Hz, 4H), 5.23 (s, 4H), 3.10 (s, 6H), 2.51 (t, $J = 7.2$ Hz, 4H), 2.06 (quin, $J = 7.2$ Hz, 2H). ^{13}C NMR (100 MHz, $CDCl_3$) δ (ppm): 172.1 (u), 167.5 (u), 163.9 (u), 140.7 (u), 131.8 (u), 128.7 (dn), 128.3 (dn), 65.8 (u), 33.3 (u), 21.3 (dn), 20.2 (u). IR $\tilde{\nu}$ (cm^{-1}): 2926, 1733, 1612, 1401, 1364, 1285, 1147, 1089, 984, 955, 887, 796, 615. Elemental analysis: expected C 59.99, H 4.83, N 22.39, O 12.79, found C 60.74, H 4.87, N 20.06. UV/vis (CH_2Cl_2): $\lambda_{max} = 320$ nm, $\lambda_{secondary peak} = 545$ nm.

General SCNP synthesis

PS(Nb) polymer was dissolved in DMF at a concentration of 0.01 M of Nb groups, and added at 1 mL/h to a solution of **Tz–Tz** in DMF (0.5 eq. relative to Nb groups on the polymer, volume equivalent to the volume of polymer solution added) held at 80 °C. The solution was stirred for 24 h at 80 °C, before being cooled to room temperature and an excess of bicyclo[2.2.1]hept-2-ene (norbornene) added to quench any remaining tetrazine. DMF was removed *in vacuo* and the SCNPs isolated by precipitation once from cold MeOH and once from cold hexanes.

Conclusions

We have shown that the tetrazine-norbornene reaction can be used, *via* a bifunctional tetrazine crosslinker and norbornene-decorated polystyrene, to form SCNPs of a diameter below 10 nm. A range of linear polymers with varying molecular weights (10 kDa and above) and incorporations of Nb units (5-20 mol%) were found to form SCNPs, albeit with a small amount of polymer-polymer coupling in all cases. Analysis of the SCNP formed from a ~ 30 kDa polymer with 20% Nb incorporation showed discrete particles by AFM and TEM, and some evidence of spontaneous aggregation in solution by SANS, SLS and DLS, which could be reversed by heating. This method of forming SCNPs by the Tz-Nb reaction confers some of the benefits of that reaction – namely, the ability to carry it out in air with no added reagents or catalysts, which simplifies synthesis and purification of the SCNPs significantly. That the reaction in this case required elevated temperatures is a drawback that could be overcome using a more reactive tetrazine crosslinker, with the aim to reduce the reaction temperature to ambient. This could then be used to form nanostructures of further complexity with the SCNPs either pre- or post-formation, such as conjugation to temperature- or reagent-sensitive substrates.

Notes and references

[a] Department of Chemistry, University of Warwick, Gibbet Hill Road, Coventry CV4 7AL, UK. Tel: +44 (0) 247 652 3236; E-mail: R.K.O-Reilly@warwick.ac.uk

1. P. Taranekar, J.-Y. Park, D. Patton, T. Fulghum, G. J. Ramon and R. Advincula, *Adv. Mater.*, 2006, **18**, 2461-2465.
2. K.-S. Park, D.-y. Kim, S.-k. Choi and D. H. Suh, *Jpn. J. Appl. Phys., Part 1*, 2003, **42**, 3877-3880.
3. D. Mecerreyes, V. Lee, C. J. Hawker, J. L. Hedrick, A. Wursch, W. Volksen, T. Magbitang, E. Huang and R. D. Miller, *Adv. Mater.*, 2001, **13**, 204-208.
4. E. Harth, B. V. Horn, V. Y. Lee, D. S. Germack, C. P. Gonzales, R. D. Miller and C. J. Hawker, *J. Am. Chem. Soc.*, 2002, **124**, 8653-8660.
5. C. T. Adkins, H. Muchalski and E. Harth, *Macromolecules*, 2009, **42**, 5786-5792.
6. T. A. Croce, S. K. Hamilton, M. L. Chen, H. Muchalski and E. Harth, *Macromolecules*, 2007, **40**, 6028-6031.

7. M. Ergin, B. Kiskan, B. Gacal and Y. Yagci, *Macromolecules*, 2007, **40**, 4724-4727.

8. P. Wang, H. Pu and M. Jin, *J. Polym. Sci., Part A: Polym. Chem.*, 2011, **49**, 5133-5141.

9. X. Jiang, H. Pu and P. Wang, *Polymer*, 2011, **52**, 3597-3602.

10. L. Oria, R. Aguado, J. A. Pomposo and J. Colmenero, *Adv. Mater.*, 2010, **22**, 3038-3041.

11. A. R. de Luzuriaga, N. Ormategui, H. J. Grande, I. Odriozola, J. A. Pomposo and I. Loinaz, *Macromol. Rapid Comm.*, 2008, **29**, 1156-1160.

12. I. Perez-Baena, I. Loinaz, D. Padro, I. Garcia, H. J. Grande and I. Odriozola, *J. Mater. Chem.*, 2010, **20**, 6916-6922.

13. A. Sanchez-Sanchez, I. Asenjo-Sanz, L. Buruaga and J. A. Pomposo, *Macromol. Rapid Comm.*, 2012, **33**, 1262-1267.

14. J. He, L. Tremblay, S. Lacelle and Y. Zhao, *Soft Matter*, 2011, **7**, 2380-2386.

15. G. Njikang, G. Liu and S. A. Curda, *Macromolecules*, 2008, **41**, 5697-5702.

16. B. Zhu, S. Sun, Y. Wang, S. Deng, G. Qian, M. Wang and A. Hu, *J. Mater. Chem., C*, 2013, **1**, 580-586.

17. B. Zhu, G. Qian, Y. Xiao, S. Deng, M. Wang and A. Hu, *J. Polym. Sci., Part A: Polym. Chem.*, 2011, **49**, 5330-5338.

18. B. Zhu, J. Ma, Z. Li, J. Hou, X. Cheng, G. Qian, P. Liu and A. Hu, *J. Mater. Chem.*, 2011, **21**, 2679-2683.

19. A. E. Cherian, F. C. Sun, S. S. Sheiko and G. W. Coates, *J. Am. Chem. Soc.*, 2007, **129**, 11350-11351.

20. J. B. Beck, K. L. Killops, T. Kang, K. Sivanandan, A. Bayles, M. E. Mackay, K. L. Wooley and C. J. Hawker, *Macromolecules*, 2009, **42**, 5629-5635.

21. P. T. Dirlam, H. J. Kim, K. J. Arrington, W. J. Chung, R. Sahoo, L. J. Hill, P. J. Costanzo, P. Theato, K. Char and J. Pyun, *Polym. Chem.*, 2013, **4**, 3765-3773.

22. R. A. Carboni and R. V. Lindsey, Jr., *J. Am. Chem. Soc.*, 1959, **81**, 4342-4346.

23. J. Sauer, D. K. Heldmann, J. Hetzenegger, J. Krauthan, H. Sichert and J. Schuster, *Eur. J. Org. Chem.*, 1998, **1998**, 2885-2896.

24. M. T. Taylor, M. L. Blackman, O. Dmitrenko, J. M. Fox, *J. Am. Chem. Soc.* 2011, **133**, 9646-9649.

25. N. Devaraj, S. Hilderbrand, R. Upadhyay, R. Mazitschek, R. Weissleder, *Angew. Chem., Int. Ed.* 2010, **49**, 2869-2872.

26. K. Lang, L. Davis, J. Torres-Kolbus, C. Chou, A. Deiters, J. W. Chin, *Nature Chem* 2012, **4**, 298-304.

27. I. A. Barker, D. J. Hall, C. F. Hansell, F. E. Du Prez, R. K. O'Reilly and A. P. Dove, *Macromol. Rapid Comm.*, 2011, **32**, 1362-1366.

28. C. F. Hansell, P. Espeel, M. M. Stamenovic, I. A. Barker, A. P. Dove, F. E. Du Prez and R. K. O'Reilly, *J. Am. Chem. Soc.*, 2011, **133**, 13828-13831.

29. C. F. Hansell and R. K. O'Reilly, *ACS Macro Lett.*, 2012, **1**, 896-901.

30. M.L. Blackman, M. Royzen, M, J. M. Fox, *J. Am. Chem. Soc.* 2008, **130**, 13518-13519.

31. M. Wiessler, W. Waldeck, C. Kliem, R. Pipkorn, K. Braun, *Int. J. Med. Sci*. 2010, **7**, 19-28

32. N. Devaraj, R. Weissleder, *Acc. Chem. Res.*, 2011, **44**, 816–827.

33. J. Schoch, M. Wiessler, A. Jäschke, *J. Am. Chem. Soc.* 2010, **132**, 8846-8847.

34. L. Chen, W. A. Phillip, E. L. Cussler and M. A. Hillmyer, *J. Am. Chem. Soc.*, 2007, **129**, 13786-13787.

35. J. Yang, M. R. Karver, W. Li, S. Sahu and N. K. Devaraj, *Angew. Chem., Int. Ed.*, 2012, **51**, 5222-5225.

36. L. Chen and M. A. Hillmyer, *Macromolecules*, 2009, **42**, 4237-4243.

37. J. A. Pomposo, I. Perez-Baena, L. Buruaga, A. Alegria, A. J. Moreno and J. Colmenero, *Macromolecules*, 2011, **44**, 8644-8649.

38. J. W. Liu, M. E. Mackay and P. M. Duxbury, *Macromolecules*, 2009, **42**, 8534-8542.

39. J. P. Patterson, A. M. Sanchez, N. Petzetakis, T. P. Smart, T. H. Epps III, I. Portman, N. R. Wilson and R. K. O'Reilly, *Soft Matter*, 2012, **8**, 3322-3328.